DISCRETE AND CONTINUOUS
DYNAMICAL SYSTEMS
Volume **6**, Number **1**, January **2000** pp. **1–20**

MODELS FOR INTERNAL WAVES IN DEEP WATER

Henrik Kalisch

Department of Mathematics
University of Texas, Austin, TX 78712, USA

Jerry L. Bona

Department of Math. and Texas Institute for Computational & Applied Math.
University of Texas, Austin, TX 78712, USA

Abstract. We study properties of solitary-wave solutions of three evolution equations arising in the modeling of internal waves. Our experiments indicate that broad classes of initial data resolve into solitary waves, but also suggest that solitary waves do not interact exactly, thus suggesting two of these equations are not integrable. In the course of our numerical simulations, interesting meta-stable quasi-periodic structures have also come to light.

1. **Introduction.** In this paper, consideration is given to long-crested unidirectional waves at the interface of a two-layer system of incompressible inviscid fluids. The top layer is assumed to be infinitely deep, while the heavier bottom layer has a finite depth h. Attention is restricted to waves whose wavelength λ is large compared to the depth h of the lower layer, and whose amplitude a is small compared to h. Moreover, the two small quantities $\frac{h}{\lambda}$ and $\frac{a}{h}$ are supposed to be of the same order. Let (x, y, z) connote a standard Cartesian coordinate system with z the vertical direction and $z = 0$ located at the interface between the two fluids in their rest position. In this situation, the Benjamin-Ono equation,

$$u_t + u_x + uu_x - Hu_{xx} = 0, \tag{1.1}$$

was first proposed by Benjamin [5] as an approximate model equation for waves on the interface whose primary direction of propagation is that of increasing values of x, which do not vary significantly in the y-direction, and for which the effects of surface tension, viscosity and molecular diffusion may be safely ignored. As mentioned, x is proportional to distance in the direction of propagation, t is proportional to elapsed time and $u(x, t)$ is proportional to the vertical deviation of the interface from its rest position at the point x at time t. The operator H is the Hilbert transform applied

1991 *Mathematics Subject Classification.* 35S10, 35Q53, 37K10, 45K05, 47G20, 65M70, 76B25, 76B55.

Key words and phrases. Nonlinear Waves, Solitons, Integro-differential Equations, Spectral Methods, Solitary-Wave Interaction.

Research partially supported by the National Science Foundation, USA.

in the spatial variable. In the derivation of (1.1), when the variables u, x and t are non-dimensional and scaled so that the dependent variable and its derivatives are of order one, (1.1) takes the revealing form

$$u_t + u_x + \epsilon u u_x - \epsilon H u_{xx} = O(\epsilon^2), \tag{1.2}$$

where ϵ is of order $\frac{h}{\lambda} \cong \frac{a}{h}$ and the $O(\epsilon^2)$ connotes terms in the formal approximation which are of quadratic or higher order in ϵ. The Benjamin-Ono equation obtains by disregarding all terms of higher order in ϵ. It follows in particular that

$$u_t + u_x = O(\epsilon), \tag{1.3}$$

and the small parameter ϵ appearing in the equation shows the dispersive term Hu_{xx} and the nonlinear term uu_x to be corrections of the same order to the basic uni-directional hyperbolic operator $u_t + u_x = 0$. Under the assumption that differentiation does not alter the ϵ-order of the dependent variable, (1.3) implies that

$$H u_{xx} + H u_{xt} = O(\epsilon),$$

so that Hu_{xx} may be replaced by $-Hu_{xt}$ in (1.2) to obtain

$$u_t + u_x + \epsilon u u_x + \epsilon H u_{xt} = O(\epsilon^2).$$

Again, disregarding terms of higher order and then rescaling, there appears the alternative model

$$u_t + u_x + u u_x + H u_{xt} = 0. \tag{1.4}$$

This equation will be termed the regularized Benjamin-Ono equation. As shown above, it is formally equivalent to the Benjamin-Ono equation. A rigorous comparison made in [2] and [10] between solutions of (1.1) and (1.4) corresponding to the same, small-amplitude, long-wavelength initial data shows the formal expectations regarding the size of the difference are met in practice over the long time scales relevant to such models.

For the situation when surface tension cannot be ignored, Benjamin [6] later derived what is now known as the Benjamin equation

$$u_t + u_x + u u_x - H u_{xx} - T u_{xxx} = 0. \tag{1.5}$$

In this equation, T is a constant proportional to the surface tension at the interface. In the present paper, the primary focus is on the dynamical properties of the solitary-wave solutions of (1.1), (1.4) and (1.5). Following remarks in Section 2 about the mathematical theory for the initial-value problems associated to the evolution equations in view, we study the resolution of an initial wave profile into solitary waves and the interaction of solitary waves. Our experiments show that all three of these evolution equations feature resolution into solitary waves in much the same way as does the Korteweg-deVries equation. Observe that equation (1.5) is a hybrid between the Korteweg-deVries and the Benjamin-Ono equation. Since both of these appear to constitute infinite-dimensional integrable systems, the question

naturally arises as to whether or not the same is true for the Benjamin equation. Section 3 contains some numerical results which indicate a negative answer to this question. For the regularized Benjamin-Ono equation, previous experience with the the regularized long wave or BBM equation

$$u_t + u_x + uu_x - u_{xxt} = 0$$

suggests that (1.4) is not integrable (cf. [9]). The numerical experiments reported here are consistent with this supposition. Finally, we observe an interesting phenomenon, namely what appears to be solutions of the Benjamin equation which at least over certain time scales consist of two or more leap-frogging solitary waves.

2. **Well-Posedness Results.** As usual, an initial-value problem

$$\begin{aligned} u_t + A(u) &= 0, \\ u(0) &= u_0, \end{aligned} \tag{2.1}$$

is well-posed in a Banach space X if corresponding to every $u_0 \in X$, there is a $T = T(\|u_0\|_X) > 0$ and a unique element $u \in C([0,T], X)$ satisfying $u(\cdot, 0) = u_0$, such that for each $t \in [0,T]$, $A(u)$ has a suitable sense and the evolution equation is satisfied at least in a weak sense. Here and below, the symbol $C([0,T], X)$ denotes the space of functions which are continuous in time and take values in the Banach space X. It is usually also required that the correspondence $u_0 \longmapsto u$ be continuous from X to $C([0,T], X)$. The initial-value problem (2.1) is globally well posed if T can be taken arbitrarily large. Not only are local and global well-posedness results a central theoretical issue for evolution equations, but they also play an important role in obtaining error estimates for numerical approximations of solutions. To describe the situation regarding (1.1), (1.4) and (1.5), we introduce some function classes. For $1 \leq p < \infty$, the space $L^p = L^p(\mathbb{R})$ is the set of measurable real-valued functions of a real variable whose p^{th} powers are integrable over $\mathbb{R}$. If $f \in L^p$, its norm is denoted $|f|_p$. The inner product in L^2 is denoted $(\cdot, \cdot)_2$. For $s \geq 0$, the space H^s is the subspace of $L^2(\mathbb{R})$ consisting of functions such that

$$\|f\|_s^2 = \int_{-\infty}^{\infty} (1 + |\xi|^2)^s |\hat{f}(\xi)|^2 d\xi < +\infty,$$

with the circumflex connoting the Fourier transform. Equivalently,

$$\|f\|_s = |J^s f|_2,$$

where $J^s = (I - \triangle)^{\frac{s}{2}}$ is the Bessel potential of order s. The space $L^\infty(\mathbb{R})$ consists of all measurable, essentially bounded functions on $\mathbb{R}$ with norm $|f|_\infty = ess\ \sup_x |f(x)|$. We shall also briefly refer to the spaces $L^\infty(0,T,X)$ of Borel measurable, essentially bounded functions on $[0,T]$ with values in X. Well-posedness and smoothing results for $X = H^s$ with $s \geq \frac{3}{2}$ for the initial-value problem associated to (1.1) were provided by Abdelouhab *et. al.* [1] , Ponce [17], [18] and Tom [20]. The Benjamin equation was proven to be well posed in L^2 by Linares [13].

These results provide a global theory because of the conservation laws which hold for these equations.

For the regularized Benjamin-Ono equation, we sketch the proof of well-posedness of the initial-value problem on the real line. Rewriting (1.4) in the form

$$(1 + H\partial_x)u_t + u_x + uu_x \quad = \quad 0$$

leads to the formally equivalent integral equation

$$u_t = K * \left(u + \tfrac{1}{2}u^2\right), \tag{2.2}$$

where K is given explicitly in terms of its Fourier transform, *viz.*

$$\hat{K}(\xi) = \frac{-i\xi}{1 + |\xi|}.$$

Upon integration with respect to t and imposition of the initial condition $u(\cdot, 0) = g$, there appears

$$u(x,t) = g(x) + \int_0^t \left\{K * (u + \tfrac{1}{2}u^2)(x,\tau)\right\}\ d\tau \tag{2.3}$$

for $x \in \mathbb{R}$ and $t > 0$. Using the fact that $H^s(\mathbb{R})$ is a Banach algebra for $s > \frac{1}{2}$, a contraction argument in the Banach space $C\left([0,t_0], H^s\right)$ with $s > \frac{1}{2}$ yields a solution over a limited time interval $[0,t_0]$. The proof shows that t_0 depends on $\|g\|_s$ like an inverse power and that the solution is unique and depends continuously on the initial data g. Thus the initial-value problem is locally well-posed in H^s for any $s > \frac{1}{2}$. To extend this solution to an arbitrary time interval $[0,T]$, *a priori* estimates are needed. The following lemma is useful in deriving the required estimates. (A discussion of these results may be found in [18].)

Lemma 1. *Let s, s_0 and s_1 be non-negative. There exist constants c_1 and c_2 depending only on s, s_0 and s_1, such that*

$$|J^s(fg) - fJ^s g|_2 \le c_1\Big\{\,|f_x|_\infty\ |J^{s-1}g|_2 + |J^s f|_2\ |g|_\infty\Big\} \tag{2.4}$$

$$|J^s f|_2 \le c_2 |J^{s_0} f|_2^{\theta}\ |J^{s_1} f|_2^{1-\theta}, \tag{2.5}$$

where $s = \theta s_0 + (1-\theta)s_1$.

Theorem. *Let $s \ge \frac{3}{2}$. If $u \in C([0,T], H^s)$ is a solution of (1.4) in the sense of distributions on $\mathbb{R} \times [0,T]$, then there are constants C and $C_s = C(\|u(\cdot,0)\|_s)$ such that*

$$\sup_{0\le t\le T} \|u(\cdot,t)\|_s^2 \le C_s e^{CT}. \tag{2.6}$$

For the proof of this theorem, a preliminary lemma is needed.

Lemma 2. *If u is a solution of (1.4) in the sense of distributions and u lies in $C([0,T], H^s)$ for some $s > \frac{1}{2}$, then for all $t \in [0,T]$,*

$$\|u(\cdot,t)\|_{\frac{1}{2}} = \|u(\cdot,0)\|_{\frac{1}{2}}. \tag{2.7}$$

Proof: Since $u \in C([0,T], H^s)$ with $s > \frac{1}{2}$, each term in the differential equation is a tempered distribution. It follows that (2.2) holds for u, and hence that $u \in C^1([0,T], H^s)$. Let $\{u_n\}_{n=1}^{\infty}$ be a sequence in $C^1([0,T], H^\infty)$ converging to u in $C^1([0,T], H^s)$, and let

$$F : C^1([0,T], H^s) \to C([0,T], H^{s-1})$$

be defined by

$$F(v) = v_t + Hv_{xt} + v_x + vv_x. \tag{2.8}$$

Since u solves (1.4), $F(u_n) \to 0$ as $n \to \infty$ in $C([0,T], H^{s-1})$ and hence $\langle u_n, F(u_n)\rangle \to 0$ as $n \to \infty$ in $C([0,T])$, where $\langle \cdot, \cdot \rangle$ connotes $H^{\frac{1}{2}}$-$H^{-\frac{1}{2}}$ duality. Since u_n is smooth for each n, it is elementary to compute that

$$2\langle u_n, F(u_n)\rangle = \frac{d}{dt}\|u_n(\cdot,t)\|^2_{\frac{1}{2}}.$$

Hence, for each $t \in [0,T]$, we have

$$\|u_n(\cdot,t)\|^2_{\frac{1}{2}} = \|u_n(\cdot,0)\|^2_{\frac{1}{2}} + 2\int_0^t \langle u_n, F(u_n)\rangle ds.$$

Taking the limit as $n \to \infty$ in the last formula gives the desired result.

Proof of the Theorem: To establish the estimate in the case $s = \frac{3}{2}$, approximate a solution u in the space $C^1([0,T], H^{\frac{3}{2}})$ by a sequence $\{u_n\}_{n=1}^{\infty}$ taken from $C^1([0,T], H^\infty)$ as above. Then $F(u_n) \to 0$ in $C([0,T], H^{\frac{1}{2}})$ and $\{\partial_x^2 u_n\}_{n=1}^{\infty}$ is bounded in $C([0,T], H^{-\frac{1}{2}})$. Consequently, $\langle F(u_n), \partial_x^2 u_n\rangle \to 0$ as $n \to \infty$ in $C([0,T])$. On the other hand, since u_n is smooth,

$$2\langle F(u_n), \partial_x^2 u_n\rangle = \frac{d}{dt}\|\partial_x u_n(\cdot,t)\|^2_{\frac{1}{2}} + \int_{-\infty}^{\infty} [\partial_x u_n(x,t)]^3 dx. \tag{2.9}$$

The Sobolev inequality and (2.5) imply there is a positive constant c_4 such that for $f \in H^{\frac{3}{2}}$,

$$\int_{-\infty}^{\infty} [\partial_x f(x)]^3 dx = |\partial_x f|_3^3 \le c_3 \|\partial_x f\|^3_{\frac{1}{6}} \le c_3 \|f\|^3_{\frac{7}{6}} \le c_4 \|f\|_{\frac{1}{2}} \|f\|^2_{\frac{3}{2}}, \tag{2.10}$$

where $c_4 = c_2 c_3$ and c_3 is another Sobolev constant. Using (2.10) in (2.9), integrating the result with respect to t and adding (2.7) leads to the inequality

$$\begin{aligned} \|u_n(\cdot,t)\|^2_{\frac{3}{2}} &\le \|u_n(\cdot,t)\|^2_{\frac{1}{2}} + \|\partial_x u_n(\cdot,t)\|^2_{\frac{1}{2}} \\ &\le \|u_n(\cdot,0)\|^2_{\frac{1}{2}} + \|\partial_x u_n(\cdot,0)\|^2_{\frac{1}{2}} \\ &\quad + c_4 \int_0^t \|u_n(\cdot,0)\|_{\frac{1}{2}} \|u_n(\cdot,s)\|^2_{\frac{3}{2}} ds + 2\int_0^t \langle F(u_n), \partial_x^2 u_n\rangle ds. \end{aligned}$$

Taking the limit as $n \to \infty$ yields

$$\|u_n(\cdot,t)\|^2_{\frac{3}{2}} \le 2\|u_n(\cdot,0)\|^2_{\frac{3}{2}} + c_4 \int_0^t \|u(\cdot,s)\|^2_{\frac{3}{2}} ds. \tag{2.11}$$

Finally, Gronwall's lemma implies (2.6) with $C = c_4$ and $C_{\frac{3}{2}} = 2\|u_n(\cdot,0)\|^2_{\frac{3}{2}}$. The general case follows from the the case $s = \frac{3}{2}$ and an inductive argument. Suppose the estimate (2.6) holds for some $r_0 \geq \frac{3}{2}$, let $s = r_0 + \alpha$, where $0 < \alpha \leq \frac{1}{2}$ and let $r = s - \frac{1}{2}$. As before, the solution u can be approximated by a sequence of smooth functions $\{u_n\}_{n=1}^{\infty}$. Calculations can be made with the u_n, and a limiting argument applied to show that the resulting inequalities actually hold for u. The limiting argument is just as it appeared for the case $s = \frac{3}{2}$, and so this procedure is abbreviated by making formal calculations with a solution u as though it had the requisite smoothness. Consider the combination

$$\langle J^r u, J^r F(u)\rangle = \langle J^r u, J^r u_t + J^r H u_{xt}\rangle + \langle J^r u, J^r u_x\rangle + \langle J^r u, J^r(uu_x)\rangle.$$

Assuming that u is a smooth solution of (1.4), there follows the relation

$$\begin{aligned}
\frac{d}{dt}\langle J^r u, J^r u + J^r H u_x\rangle &= -2\langle J^r u, uJ^r u_x\rangle \ + \ 2\langle J^r u, J^r(uu_x) - uJ^r u_x\rangle \\
&\leq (J^r u, u_x J^r u)_2 \ + \ 2|J^r u|_2 \ |J^r(uu_x) - uJ^r u_x|_2 \\
&\leq (1 + 2c_1)|u_x|_\infty |J^r u|_2^2 \\
&\leq c_5\|u\|_s |J^r u|_2^2 \\
&\leq c_5\|u\|_s |J^{r_0} u|_2^2,
\end{aligned}$$

where (2.4) has been used. Integrate this with respect to t over the interval $[0,t]$ where $t \leq T$ and use the fact that $\|u\|_s$ is equivalent to $\langle J^r u, J^r u + J^r H u_x\rangle$ along with the induction hypothesis to write

$$\|u(\cdot,t)\|_s^2 \leq \|u(\cdot,0)\|_s^2 + c_5 C_{r_0} e^{CT}\int_0^t \|u(\cdot,\tau)\|_s d\tau. \tag{2.12}$$

From (2.12), the required *a priori* estimate for $\|u\|_s$ with $s = r_0 + \alpha$ follows immediately. The induction is thus complete.

Corollary. *The initial-value problem for equation (1.4) is globally well-posed in $H^s(\mathbb{R})$ for any $s \geq \frac{3}{2}$.*

Remark: It is possible to obtain existence of a weak solution of (1.4) in $L^\infty(0,\infty,H^{\frac{1}{2}})$ by a standard limiting procedure. For initial data $g \in H^{\frac{1}{2}}$, let $\{g_n\}_{n=1}^{\infty}$ be a sequence of H^∞-functions converging in $H^{\frac{1}{2}}$ to g, and let $\{u_n\}_{n=1}^{\infty}$ be the associated globally defined solutions whose existence is guaranteed by the last result. Because of (2.7), the sequence $\{u_n\}_{n=1}^{\infty}$ is bounded in $L^\infty(0,T,H^{\frac{1}{2}})$. From (2.2) and the Sobolev inequality, it follows that $\{\partial_t u_n\}_{n=1}^{\infty}$ is bounded in $L^2(0,T,L^2)$. Using a Cantor diagonalization construction and the Aubin-Lions compactness lemma [14], a subsequence $\{u_{n_k}\}_{k=1}^{\infty}$may be extracted so that

$$u_{n_k} \to u \qquad \text{weak}^* \text{ in } L^\infty(0,T,H^{\frac{1}{2}}), \tag{2.13}$$

$$\partial_t u_{n_k} \to \partial_t u \qquad \text{weak}^* \text{ in } L^\infty(0,T,L^2), \tag{2.14}$$

$$u_{n_k} \to u \qquad \text{pointwise almost everywhere in } [0,T]\times\mathbb{R}. \tag{2.15}$$

Following standard reasoning (cf. [11], [14]), it is inferred that $u \in C([0,T], L^2)$, that $u(0) = g$ and that u satisfies (1.4) in a weak sense. Moreover, it can be arranged via a further diagonalization that the same subsequence converges as in (2.13)-(2.15) for any value of $T > 0$. It follows in particular that $u \in L^\infty(0, \infty, H^{\frac{1}{2}})$.

3. **Numerical Results.** Since the operators appearing in the linear part of the equations featured here may be interpreted as Fourier multiplier operators, it is convenient to use a Fourier-Collocation method to effect a spatial discretization. This forces periodic boundary conditions, hence a large spatial domain is needed to simulate the problem on the real line. The nonlinear terms are handled pseudo-spectrally, which is to say they are evaluated in physical space. The details of the numerical scheme together with a convergence study are given in the Appendix. Here, we focus on the numerical experiments. For numerical study, we put the Benjamin equation in the normalized form

$$u_t + uu_x + Hu_{xx} + u_{xxx} = 0. \tag{3.1}$$

This form of the equation reverses the sense of time. However, the structure of the equation is unchanged since the dispersion relation is odd.

Resolution Properties

As a choice of initial waveform, we use a two-parameter family of Gaussian functions

$$u(x,0) = Ae^{-\left(\frac{x}{\lambda}\right)^2} \tag{3.2}$$

where A represents the amplitude and λ the wavelength. The evolution according to the Benjamin-Ono and regularized Benjamin-Ono equations is shown in Figures 1 and 3. In these figures, the height u of the wave profile is graphed against the x-axis at $t = 0$ and at successive times. In Figure 1, observe that the Gaussian disintegrates into one solitary wave and an oscillatory tail for both the Benjamin-Ono and the regularized Benjamin-Ono equation when $\lambda = 4$. Raising λ to 6 results in two solitary waves in both equations; however, the second solitary wave for the regularized equation in Figure 3 has significantly smaller amplitude than its Benjamin-Ono counterpart. Increasing A seems to only affect the height and width of the emerging solitary waves. Figures 2 and 4 show the evolution according to the Benjamin equation. Three solitary waves emerge if $A = 2$ and $\lambda = 4$, demonstrating that solutions to the Benjamin equation behave quite differently from correspondingly initiated solutions of the Benjamin-Ono equation. When $\lambda = 6$, there emerges a pair of "orbiting" solitary waves. The evolution of a pair of such waves may be described as follows. At first, the leading wave is taller than the trailing wave, so it seems that it should outpace the smaller wave and separate. However, just before that happens, the leading wave loses height and speed. This loss is picked up by the trailing wave which now grows taller and faster, thereby gaining upon the leading wave. It comes to a near interaction, but just before the trailing wave begins to pass the leading wave, it in turn looses height and speed and falls behind again. Although not visible in Figure 4, after this near interaction,

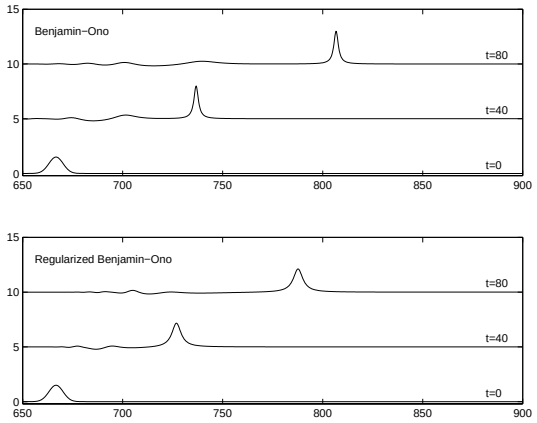

FIGURE 1. Evolution of initial data as in (3.2) with $A = 2$ and $\lambda = 4$.

the shedding of a small dispersive tail is observed. Increasing λ results in resolution into a doublet as just described together with more single solitary waves up to a point where instead of the leading state being a leap-frogging pair, a triplet of orbiting solitary waves along with the same number of detached single solitary waves emerges. Increasing λ further increases the number of single solitary waves, but ultimately a quadruple of orbiting solitary waves emerges. It cannot be said with certainty that these orbiting solitary waves represent a dynamically stable state of the system. Indeed, we observed that on occasion one of a group of five or more orbiting solitary waves separated from the rest after some time. It seems possible that after a long enough time, even the pair of orbiting solitary waves will separate. In fact, we followed the evolution of a pair of bound solitary waves for a long time and observed that the maximum separation of the two, occurring when their amplitudes are identical, increases over time. This strongly suggests that the two leap-frogging solitary waves represent an intermediate state of the system which may eventually transform into two separately propagating solitary waves. This point warrants further numerical and analytical investigation.

Solitary Waves

For the Benjamin-Ono equation, Benjamin [5] found solitary-wave solutions in the form

$$\phi_d(y) = \frac{4d}{1 + d^2 y^2}, \tag{3.3}$$

for any $d > 0$. Solitary waves for the regularized equation can be obtained by a simple rescaling, viz.

$$\phi_d(y) = \frac{4d}{1 + (\frac{d}{d+1})^2 y^2}. \tag{3.4}$$

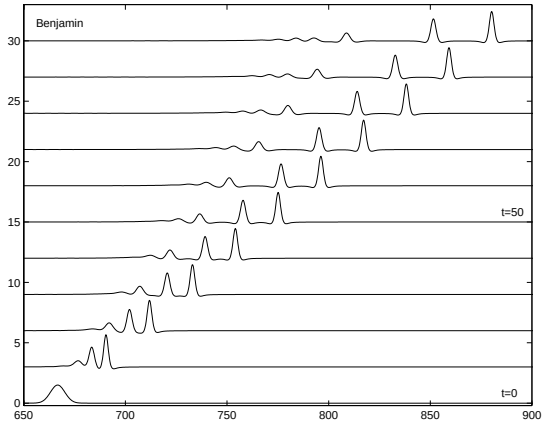

FIGURE 2. Evolution of initial data as in (3.2) with $A = 2$ and $\lambda = 4$.

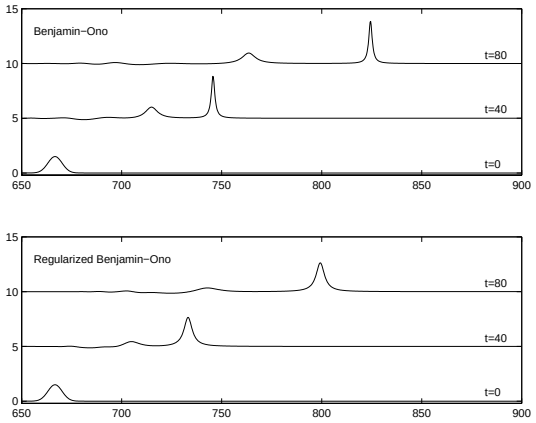

FIGURE 3. Evolution of initial data as in (3.2) with $A = 2$ and $\lambda = 6$.

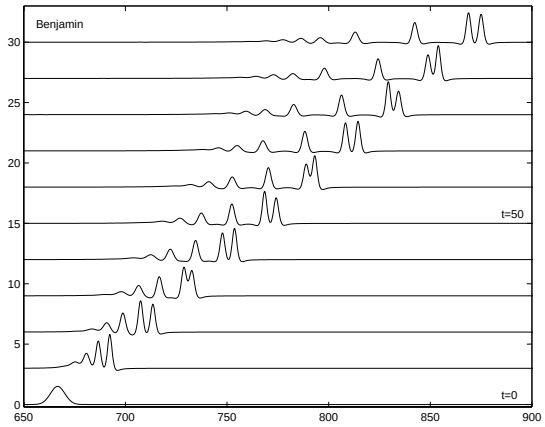

FIGURE 4. Evolution of initial data as in (3.2) with $A = 2$ and $\lambda = 6$.

These exact solutions were used to test our numerical schemes (see Appendix). Solitary-wave solutions of the Benjamin equation satisfy the equation

$$-\phi + \phi^2 + 2\gamma H\phi' + \phi'' = 0, \tag{3.5}$$

where

$$\gamma = \frac{1}{2\sqrt{c}}$$

and $c > 0$ is the wavespeed. Exact solutions are not currently available. However, it has been shown (see [3], [4] and [12]) that there exists a family of stable solitary waves with $0 \leq \gamma < 1$. The extremal $\gamma = 0$ corresponds to the solitary wave of the Korteweg-deVries equation. In [3], Albert *et. al.* used a continuation technique to approximate solutions of (3.5). Tuck and Wiryanto [21] performed numerical constructions comparing solutions of (3.5) to solutions of the full Euler equations. In this report, we use a technique favored by Bona and Chen [8] to generate approximate solitary waves utilizing the time-dependent code. The technique can be explained as follows. As observed in the last section, certain initial data evolve into a train of solitary waves. Attention is focused on one of those and the rest are manually deleted from the solution profile. The stripped profile is not in fact a solitary wave, and upon evolving further in time it sheds a dispersive tail. After the tail separates from the solitary wave, it is deleted, the solitary wave translated to the left and the result used as initial data. This procedure is repeated a number of times, resulting in due course in a very good approximation to a solitary wave. To gain some confidence in the approximate solutions generated by this procedure, a quantitative analysis of their properties is presented in Tables 1 and 2. These tables feature data related to two approximate solutions of (3.5) with $\gamma \sim 0.3551$ and $\gamma \sim 0.7267$, respectively. These waves were used as initial data in our evolution code, integrated over the time interval $[0, T]$ with $T = 30$, and several aspects of the results monitored to understand just how close the solutions are to true solitary waves. One question in this direction is how well the approximations resemble the exact solitary waves in shape. To understand this, we determine the shape error as follows: integrate the approximate solitary wave to a time T, use a spline interpolation to find the peak, and translate the profile back so that the peak is in its original position. Then compare the result with the initial waveform in the L^∞- and the L^2-norm. As can be seen in Table 1, the error in shape is on the order of 10^{-3}. For the definition of the L^2- and the L^∞-error, see the Appendix. The maximal error in height and energy is about 10^{-5}. This calculation was done on the spatial domain $[0, 3200]$ using $N = 8192$ Fourier modes and a time step $k = 0.004$. As a reference, we repeated the same calculation with an exact solitary wave for the Benjamin-Ono equation, obtaining similar results. However, choosing the time step and the grid size smaller, it was possible to decrease the error in the Benjamin-Ono situation, whereas for the approximate Benjamin solitary waves, this was not possible. In the latter case, the size of the discrepancy is clearly limited by the error remaining from the generating procedure.

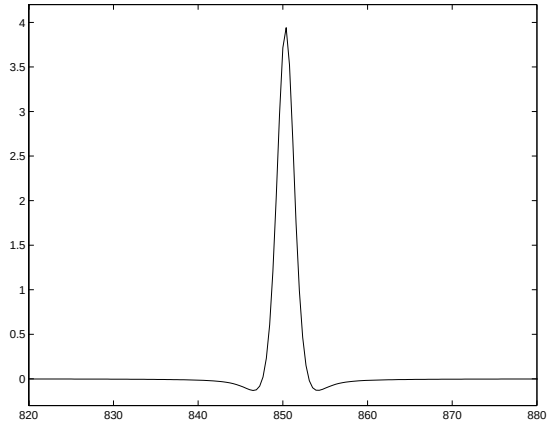

FIGURE 5. Solitary Wave for the Benjamin equation with $\gamma \sim 0.3551$.

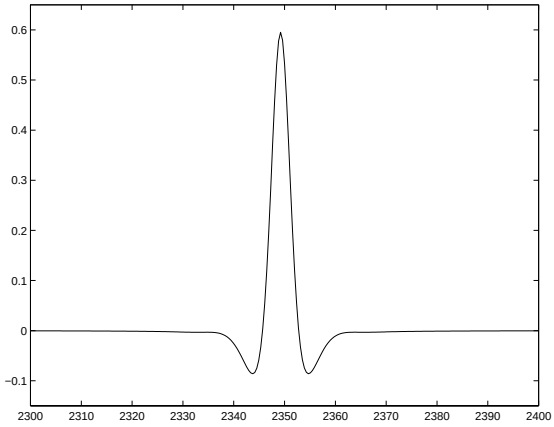

FIGURE 6. Solitary Wave for the Benjamin equation with $\gamma \sim 0.7267$.

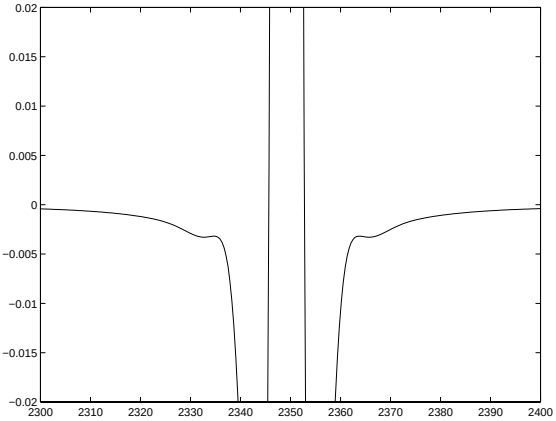

FIGURE 7. Close-up of the wave in Figure 6.

	$\gamma = 0.3551$	$\gamma = 0.7267$
L^∞	2.512e-03	2.154e-03
L^2	2.837e-03	2.685e-03

TABLE 1. Maximum error in shape up to $T = 30$ for approximate solitary- wave solutions of the Benjamin equation.

	Value	Error	Value	Error
Height	3.948	2.063e-04	0.595	9.862e-06
Energy	5.161	3.618e-07	1.024	2.075e-07
Speed	1.603	4.989e-04	0.383	2.79-e03
γ	0.3551		0.7267	

TABLE 2. Maximum error until $T = 30$ in height, energy and speed for approximate solitary waves for the Benjamin equation.

Interaction

The interaction of two solitary-wave solutions of a nonlinear dispersive evolution equation can give clues about the integrability of the equation. While the Benjamin-Ono equation is known to be integrable, our experiments indicate that both the regularized Benjamin-Ono and the Benjamin equation are not integrable. In each case, the interaction of two solitary waves is shown to leave behind an oscillatory wavetrain. For the regularized Benjamin-Ono equation, we used as the initial wave profile a solitary wave of height 1 preceded by a solitary wave of height 6. For the Benjamin equation we used the two solitary waves shown in Figures 5 and 6. In each case, the taller wave travels to the right at a higher speed, so it overtakes the smaller wave in due course. Because of the quadratic decay of the tails, it was necessary to situate the solitary waves so that the peaks were far from each other. In the experiments reported here, the peaks were separated by approximately 1600. This brought the overlap down to about 10^{-5}. Another difficulty is the artificial periodicity in the numerical approximation. To minimize this effect, the experiments were performed on a rather large domain $[0, L]$ with $L = 6400$. This was sufficient to have the decaying tail at the endpoints on the order of 10^{-5} and to follow the evolution of the waves without one of them wrapping around and reentering at the other end. The two solitary waves coalesced at about $t = 1150$. To prepare for the experiment, we tested the setup by letting a single solitary wave evolve until $t = 1200$. Since the exact form of solitary waves is known for the regularized Benjamin-Ono equation, it was possible to determine the error in this case (see Table 3). A spline interpolation showed that the error in shape is near machine precision. Similarly, for a single solitary wave evolving to $t = 1200$, the error in height is near machine precision, even when using a time step as coarse as

k	Height 1	Height 6
0.05	4.509e-5	2.272e-1
0.025	6.217e-7	7.321e-3
0.0125	5.957e-7	2.454e-4

TABLE 3. L^∞-Error for a single solitary-wave solution of the regularized Benjamin-Ono equation at T=1200.

$k = 0.05$. For the Benjamin equation, we could only determine the error between the computed solution and the approximate solitary wave we started with. For the evolution of a single solitary wave, we obtained an error similar to that shown in Tables 1 and 2, indicating that our approximate solitary waves are close to exact solitary-wave solutions and that the numerical scheme is capable of accurately making long-time integrations.

In Figures 8 and 9 some details of the interaction for the regularized Benjamin-Ono equation are shown. Note the presence of an oscillatory tail trailing behind the smaller wave after the interaction. Although not shown here, this tail is strongest right after the interaction and becomes progressively weaker as it lags behind the smaller wave and spreads out. To check the accuracy of the numerical solution in the region of the dispersive tail, we ran calculations with $k = 0.05$ and $k = 0.025$, and compared the dispersive tail in these approximations with a calculation using $k = 0.0125$. The difference was 1.184e-04 and 3.666e-06, respectively. This is better than the factor of 16 guaranteed by the 4^{th}-order convergence of the Runge-Kutta time-stepping scheme used for the regularized Benjamin-Ono equation.

In the case of the Benjamin equation, an oscillatory tail also appears after the interaction. Again, the tail lengthens, decays slowly and separates from the solitary waves. To integrate the Benjamin equation, the time step had to be quite a bit smaller. Calculations with $k = 0.008$, $k = 0.004$ and $k = 0.002$ were made, and then compared to a solution obtained using $k = 0.001$. In this case, it was observed that the difference went down by a factor of 4 which is in accordance with the 2^{nd}-order convergence of our temporal integration method for the Benjamin equation.

As a reference, we also studied the interaction of two solitary-wave solutions of the Benjamin-Ono equation using the same scheme. As expected, the interaction is clean, meaning that no dispersive tail appears after the interaction. The interaction for the Benjamin-Ono equation was also studied by Thomeé and Vasudeva Murthy [19] using a finite-difference scheme and by Dougalis and Pelloni [16] using a Fourier spectral method. In both these works, the interaction was found to be elastic.

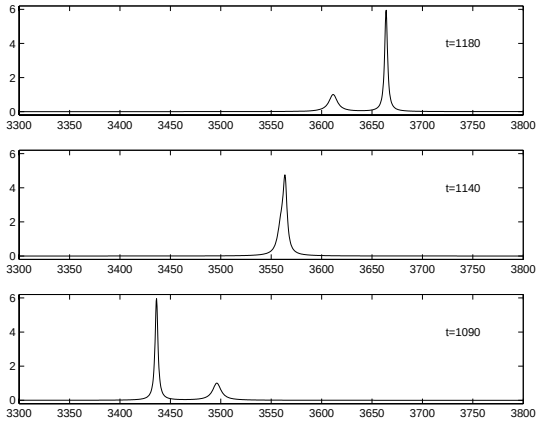

FIGURE 8. Interaction of two solitary waves for the regularized Benjamin-Ono equation.

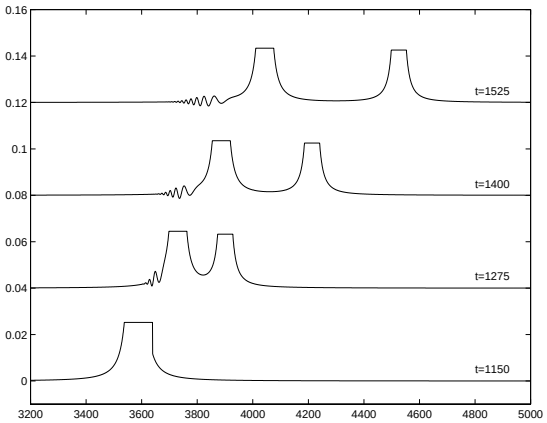

FIGURE 9. Interaction of two solitary waves for the regularized Benjamin-Ono equation; close-up of the oscillatory tail.

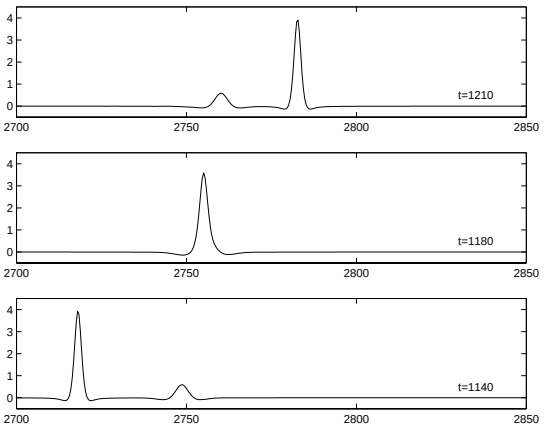

FIGURE 10. Interaction of two solitary waves for the Benjamin equation.

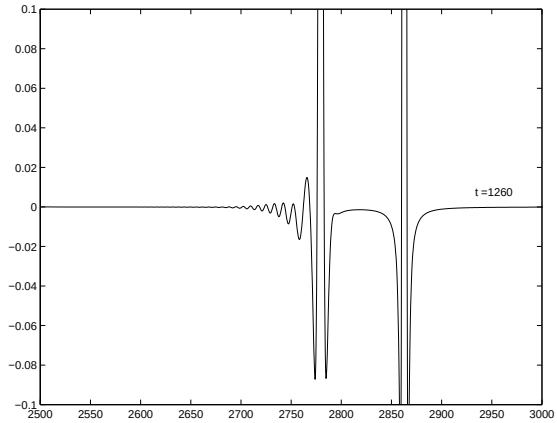

FIGURE 11. Interaction of two solitary waves for the Benjamin equation; close-up of the oscillatory tail.

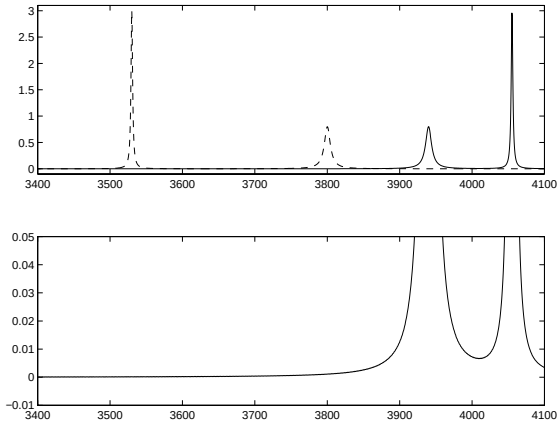

FIGURE 12. Interaction of two solitary waves for the Benjamin-Ono equation. The dashed line shows the initial data, while the solid line shows the solution profile at $t = 700$.

4. **Appendix.** The discrete Fourier transform of a function u on the interval $[0, 2\pi]$ is given by

$$\tilde{u}_n = \frac{1}{N} \sum_{j=0}^{N-1} u(x_j) e^{-inx_j},$$

where the grid points are chosen to be $x_j = \frac{2\pi j}{N}$ for $0 \leq j < N$ and $-\frac{N}{2} \leq n < \frac{N}{2} - 1$. The inverse Fourier transform is defined by

$$U_N(x) = \sum_{n=-\frac{N}{2}-1}^{\frac{N}{2}} \tilde{u}_k e^{inx}.$$

This is an exact expression at the grid points since Jackson's formula gives

$$U_N(x_j) = \sum_{n=-\frac{N}{2}}^{\frac{N}{2}} \tilde{u}_k e^{inx_j} = u(x_j),$$

so that one may think of U_N as the N^{th}-order trigonometric interpolant of u. To define the discrete Fourier transform on the interval $[0, L]$, an appropriate scaling has to be used.

The Benjamin Equation

Approximating the solution u to (3.1) by U_N, we obtain the semi-discrete equation

$$\frac{d}{dt}U_N + \tfrac{1}{2}D({U_N}^2) + HD^2(U_N) + D^3U_N = 0,$$

where D denotes the Fourier-collocation derivative. The time discretization is achieved by a Crank-Nicholson scheme for the linear part and an Adams-Bashforth method for the nonlinear term. We demonstrate the case of the Benjamin-Ono equation, dropping the subscript N for the sake of clarity. In the case of the Benjamin equation, the third-order dispersive term has to be added. Let k be size of the time step. Denoting the solution at the n^{th} time level by U^n, U^{n+1} is computed according to

$$\frac{U^{n+1} - U^n}{k} = \frac{HD^2U^{n+1} + HD^2U^n}{2} + \frac{1}{4}\left(3D(U^2)^n - D(U^2)^{n-1}\right).$$

This scheme has local truncation error of order k^2, so that second-order convergence is expected. This expectation is confirmed by the results described in Table 4. The norm used to calculate the error is the normalized discrete L^2-norm

$$\|u\|_{N,2}^2 = \frac{1}{N}\sum_{i=1}^{N} |u(x_i)|^2.$$

The L^2-error is then defined to be

$$E_2 = \frac{\|u - U\|_{N,2}}{\|u\|_{N,2}},$$

The L^∞-norm is

$$\|u\|_{N,\infty} = \max_{1\le i\le N} |u(x_i)|,$$

and the L^∞-error is

$$E_\infty = \frac{\|u - U\|_{N,\infty}}{\|u\|_{N,\infty}}.$$

We used the exact solitary-wave solution of the Benjamin-Ono equation (3.3) with $d = 0.5$ on a domain $[0, L]$, where $L = 800$. For the calculations shown, 4096 grid points were used and the solution was integrated to the final time $T = 1$. The benefit of using a spectral method with the above scheme is that the highest order term can be evaluated very simply. Since the nonlinear term is treated explicitly, there is potential nonlinear instability. For the Benjamin equation, this is not a serious

k	L^∞-error	Ratio
0.1000	1.130e-1	
0.0500	2.434e-2	4.64
0.0250	5.875e-3	4.14
0.0125	1.461e-3	4.02
0.0063	3.655e-4	4.00
0.0031	9.147e-5	4.00
0.0016	2.288e-5	4.00
0.0008	5.724e-6	4.00
0.0004	1.433e-6	3.99
0.0002	3.602e-7	3.98

TABLE 4. Benjamin-Ono equation; error due to temporal discretization.

N	L^2-error	Ratio
512	1.993e-4	
1024	6.232e-5	3.20
2048	2.541e-6	24.52
4096	1.756e-9	1446.83
8192	3.001e-10	5.85

TABLE 5. Benjamin-Ono equation; error due to spatial discretization.

problem. Since the dispersive smoothing mechanism is weaker for the Benjamin-Ono equation, one has to choose more grid points and a smaller time step in this case. However, another advantage of the spectral method is that relatively few grid points are needed to obtain good spatial accuracy, so that we were able to numerically simulate the Benjamin-Ono equation without difficulty. Moreover, for smooth solutions the error due to the spatial discretization decreases exponentially. To isolate the error introduced by the spatial discretization, we chose a very small time step $k = 0.000001$ and did some calculations with varying grid size. We see exponential convergence in Table 5 until we run into the error due to the temporal discretization and the algebraic decay of the solution. The calculations shown in Table 5 are for the setup just described, except the size of the domain was doubled. Since we integrate for a long time, it is important to know how the error grows in time. From Figure 2, it is apparent that the error for the Benjamin-Ono equation grows less than quadratically with T. As mentioned before, an exact solution of the Benjamin equation is not available. To test the proposed scheme for the Benjamin equation, a calculation with time step $k = 0.0001$ was made. Several runs with much larger time steps were then made and compared to the simulation with the very fine time step. In this way an estimate of the temporal convergence rate of the scheme was obtained. The result is shown in Table 6. The number of modes in

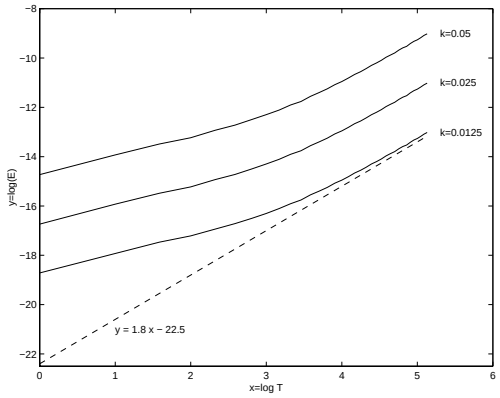

FIGURE 13. Growth of L^∞-error.

this calculation was $N = 4096$, the solution was determined up to $T = 1$ and the initial data was $u_0 = 10c^2 sech^2(c^2 x)$.

k	L^∞-error	Ratio
0.100000	6.084e-2	
0.050000	1.440e-2	4.22
0.025000	3.560e-3	4.05
0.012500	8.890e-4	4.00
0.006250	2.224e-4	4.00
0.003125	5.563e-5	4.00

TABLE 6. Benjamin equation; error due to temporal discretization.

The Regularized Benjamin-Ono Equation

To discretize the regularized version of the Benjamin-Ono equation, use is made of the equivalent formulation (2.2). There are no problems with stability as the resulting semidiscrete system is not stiff. We therefore use an explicit fourth-order Runge-Kutta scheme for the time-discretization. The Runge-Kutta algorithm has the form

$$U^{n+1} = U^n + k\frac{1}{6}\left(\Gamma_1 + \tfrac{1}{2}\Gamma_2 + \tfrac{1}{2}\Gamma_3 + \Gamma_4\right),$$

where the Γ_i are defined by

$$\begin{aligned} v_1 &= U^n & \Gamma_1 &= F(v_1) \\ v_2 &= U^n + \tfrac{1}{2}k\Gamma_1 & \Gamma_2 &= F(v_2) \\ v_1 &= U^n + \tfrac{1}{2}k\Gamma_2 & \Gamma_3 &= F(v_3) \\ v_1 &= U^n + \ \ k\Gamma_3 & \Gamma_4 &= F(v_4) \end{aligned}$$

k	L^2 -error	Ratio
0.4	2.437e-03	
0.2	1.604e-04	15.194
0.1	1.008e-05	15.917
0.05	6.344e-07	15.888
0.025	9.091e-08	6.978
0.0125	8.203e-08	1.108

TABLE 7. Regularized Benjamin-Ono ; error due to temporal discretization.

N	L^2-error	Ratio
1024	4.921e-01	
2048	2.378e-01	2.07
4096	2.125e-02	11.19
8192	1.968e-04	107.69
16384	2.431e-08	8097.02
32768	1.335e-09	1.82

TABLE 8. Regularized Benjamin-Ono equation; error due to spatial discretization.

and F is given in terms of the discrete form of the convolution operator K by $\widetilde{F(V)}_n = \frac{-in}{1+|n|}\left(\tilde{V}_n + \widetilde{(V^2)}_n\right)$. To check the algorithm, we used the exact form (3.4) of the regularized Benjamin-Ono solitary waves. A representative result for a wave of height 3 is given in Tables 7 and 8. In this calculation, the solution was approximated from $T = 0$ to $T = 3.2$ and the size of the domain was 6400. In the computations shown in Table 7, 8192 Fourier modes were used. The 4th-order convergence of the scheme is apparent up to $k = 0.025$, when the error became dominated by the spatial discretization and the artificial periodicity. Table 8 displays the spatial convergence rate for a calculation with $k = 0.0125$. We observe exponential convergence before reaching the limit set by the size of the time step and the artificial periodicity. Similar results obtain for other solitary waves with heights between 0.5 and 6. For smaller waves, a larger interval has to be used, while for taller waves, the number of Fourier modes needs to be increased.

REFERENCES

[1] L. Abdelouhab, J. L. Bona, M. Felland and J.-C. Saut, *Nonlocal models for nonlinear dispersive waves*, Physica D **40** (1989) 360-392.

[2] J.P. Albert and J.L. Bona, *Comparisons between model equations for long waves*, J. Nonlinear Sci. **1** (1991) 345-374.

[3] J.P. Albert, J.L. Bona and J.M. Restrepo, *Solitary-wave solutions of the Benjamin equation*, SIAM J. Appl. Math. **59** (1999) 2139-2161.

[4] J. Angulo, *Existence and stability of solitary-wave solutions of the Benjamin equation*, Adv. Diff. Eq. **152** (1999) 136-159.

[5] T.B. Benjamin, *Internal Waves of permanent form in fluids of great depth*, J. Fluid Mech. **29** (1967) 559-592.

[6] T.B. Benjamin, *A new kind of solitary wave*, J. Fluid Mech. **245** (1992) 401-411.

[7] T.B. Benjamin, J.L. Bona and J.J. Mahony, *Model equations for long waves in nonlinear dispersive systems*, Philos. Trans. Royal Soc. London Ser. A **272** (1972) 47-78.

[8] J.L. Bona and M. Chen, *A Boussinesq system for two-way propagation of nonlinear dispersive waves*, Physica D **116** (1998) 191-224.

[9] J. L. Bona, W.G. Pritchard and L.R. Scott, *Solitary-wave interaction*, Phys. Fluids **23** (1980) 438-441.

[10] J. L. Bona and M. Scialom, *The effect of change in the nonlinearity and the dispersion relation of model equations for long waves*, Canadian Appl. Math. Quarterly **3** (1995) 1-41.

[11] J. L. Bona and R. Smith, *The initial-value problem for the Korteweg-deVries equation*, Philos. Trans. Royal. Soc. London Ser. A **278** (1975) 555-601.

[12] H. Chen and J. L. Bona, *Existence and asymptotic properties of solitary-wave solutions of Benjamin-type equations*, Adv. Diff. Eq. **3** (1998) 51-84.

[13] F. Linares, *L^2 global well-posedness of the initial value problem associated to the Benjamin equation*, J. Diff. Eq. **152** (1999) 377–393.

[14] J.L. Lions, *Quelques methodes de résolution des problèmes aux limites non-linéares* (Dunod, Paris, 1969).

[15] T. Miloh, M. Prestin, L. Shtilman and M.P. Tulin, *A note on the numerical and N-soliton solutions of the Benjamin-Ono evolution equation*, Wave Motion **17** (1993) 1-10.

[16] B. Pelloni and V.A. Dougalis, *Numerical solution of some nonlocal, nonlinear dispersive wave equations*, preprint.

[17] G. Ponce, *Smoothing properties of solutions to the Benjamin-Ono equation*, In Analysis and Partial Differential Equations (ed. C. Sadovsky) Lecture Notes in Pure & Appl. Math. **122** Dekker: New York (1990) 667-679.

[18] G. Ponce, *On the global well-posedness of the Benjamin-Ono equation*, Diff. Integral Eq. **4** (1991) 527-542.

[19] V. Thomeé and A.S. Vasudeva Murthy, *A numerical method for the Benjamin-Ono equation*, BIT **38** (1998) 597-611.

[20] M.M. Tom, *Smoothing properties of some weak solutions of the Benjamin-Ono equation*, Diff. Integral Eq. **3** (1990) 683-694.

[21] E.O. Tuck and L.H. Wiryanto, *On steady periodic interfacial waves*, J. Engineering Math. **35** (1999) 71-84.

Received for publication November 1999.

E-mail address: bona@math.utexas.edu

E-mail address: kalisch@math.utexas.edu